PRACE NAUKOWE Wyższej Szkoły Pedagogicznej w Częstochowie
Seria: FIZYKA z. V, 2002

A. BRENIER[(1)], I.V. KITYK[(2)], J. BERDOWSKI[(2)] , A. MAJCHROWSKI[(3)]

[(1)]*Laboratoire de Physico-Chimie des Matériaux Luminescents, UMR CNRS n°5620, 10 rue Ampère, 69622 Villeurbanne, France.*
[(2)]*Institute of Physics, Pedagogical University of Częstochowa, PL-42217, Al. Armii Krajowej 13/15, Częstochowa, Poland; e-mail:i.kityk@wsp.czest.pl*
[(3)]*Institute of Applied Physics WAT, 2 Kaliskiego Str., 00-908 Warsaw, Poland.*

Nd^{3+}-doped BiB_3O_6 (BIBO) as a new potential self-frequency conversion laser crystal

1. Introduction

The bismuth triborate crystal, BiB_3O_6 (BIBO), was first grown by Liebertz in 1982–1983 [1]. Recently, high quality single crystals have been elaborated in large size by the top-seeded method [2]. The crystallographic structure is monoclinic with space group C2. It consists of sheets constituted of BO_3-triangles and BO_4-tetrahedra in the ratio 2:1, linked by six-coordinated Bi^{3+} cations [3]. The unit cell parameters are a=7.116 Å, b=4.993 Å, c=6.508 Å, β=105.62°, Z=2.

Because the crystalline structure is non-centrosymmetric, second-order nonlinear optical properties are expected and interestingly, the nonlinear optical coefficients d_{ij} were revealed to be exceptionally large, from 0.9 up to 2.8 pm/V [4–5]. These are in fact the highest values among the borate family [6] and this result can be tentatively attributed to the special influence of the Bi^{3+} cations on the dielectric response. Moreover, the linear optical properties of BIBO are such that the crystal is phase-matchable for many interactions [5], leading to promising applications in frequency conversion.

Recently, attempts have been made to dope BIBO with trivalent rare earth cations [7]. It is not easy but possible and in case of lasing, it would lead to a self-active laser crystal. These devices are of special importance because of the advantages of solid-sate technology (compactness, low maintenance...)

and could be used in a variety of applications: color projection, high density optical data storage, laser printing, medicine, argon-laser replacement, biofluorescence, underwater communications, stereo lithography, photodynamic therapy. A review of the self-active laser crystals can be found in Ref. [8].

In the present work, we have doped BIBO with Nd^{3+} ions. We exhibit the emission and absorption spectroscopy in function of the light polarization and we perform the Judd-Ofelt analysis. Low temperature spectroscopy shows that there is only one kind of Nd^{3+} emitting centre. We calculate the phase matching directions implied in self-frequency doubling, self-sum and self-difference frequency mixing, and the associated effective second-order nonlinear optical coefficient and stimulated emission cross-sections.

2. Crystal growth

According to Levin et al. [9] Bi_2O_3 and B_2O_3 form four congruently melting compounds with corresponding molar ratios of bismuth oxide and boron oxide as 2:1, 3:5, 1:3, and 1:4. BIBO (1:3) crystallises from melts having very narrow range of composition (72.5 to 77.5mol% of B_2O_3), what imposes the necessity of very precise melt synthesis. The congruent BIBO composition melts at 726°C. Very high viscosity of molten B_2O_3 (75mol% of BIBO) and its evaporation changing the composition of the melt during long processes of synthesis make it difficult to form homogeneous and stoichiometric BIBO melts. To overcome these obstacles we used the following procedure: first B_2O_3 (Merck, Suprapur) powder was molten in the platinum crucible and heated up to 1000°C to remove water. In the next step, after finding the quantity of molten B_2O_3 by weighing, proper amounts of Bi_2O_3 (ABCR, 5N) were added to molten B_2O_3 (100°C above the melting temperature of BIBO) and the mixture was stirred with specially designed platinum stirrer. The procedure allows to obtain homogeneous BIBO melt in less than 24 hours. Owing to relatively short time of synthesis B_2O_3 losses were minimised and water removed from B_2O_3 in the initial stage of the process did not influence the composition of the melt.

Enormously high viscosity of molten BIBO made it difficult to obtain seed crystals from the melt, so we used re-crystallisation of BIBO glass rods (5mm in diameter) at 600°C for several days. Obtained polycrystalline rods were used in first runs as seeds to grow small BIBO crystals, which were used as seeds in the following processes.

The crystallisation processes were carried out in two-zone resistance furnace that was controlled by two independent microprocessor controllers/programmers Eurotherm 906S. These high precision multi-zone resistance furnaces were developed in Institute of Applied Physics during investigations

of High Temperature Solution Growth (flux growth) of several oxide materials for opto-electronics like borates, sillenites, and double tungstates [10]. High heat capacity of the furnaces allowed to grow BIBO single crystals under very stable temperature conditions. The temperature inside the furnace could be changed linearly at the rates as slow as 0.01°C/h and its multi-zone construction enabled us to shape the temperature gradients in a wide range. During BIBO crystallisation neither pulling nor rotation were used, what made the segregation of constituents on the solid-liquid interface difficult, so only very slow cooling rate (0.0125°C/h) guaranteed stable growth of good quality BIBO single crystals. Owing to small temperature gradients BIBO single crystals grew in the melt on a seed introduced to the melt from the top. They were confined with flat crystallographic faces. After the growth process BIBO single crystals were withdrawn from the melt and cooled to the room temperature at 20°C/h.

In case of single crystal growth of neodymium doped BIBO single crystals (BIBO:Nd) we introduced 1at% of Nd^{3+} ions into the melt and the crystallisation was carried out on pure BIBO seeds. The dimensions of the as-grown balls were 18 X 12 X 8 mm^3. As-grown crystals had regions with some inclusions, but most of their volume was transparent and free from macroscopic defects. Becker in Ref. [7] reported that in case of Pr^{3+} and Er^{3+} BIBO doping satisfying quality of BIBO:RE single crystals can be obtained only from melts containing less than 0.1 at% of rare earth ions. In our case the concentration of Nd^{3+} ions was ten times higher. Nevertheless as-grown BIBO:Nd single crystals were colourless when observed with naked eye. Their chemical composition was analysed by electron microprobe analysis (EPMA) using the JEOL JXA-8621MX at Tohoku University and was found to be: 10.72 atom% for Bi^{3+} and 0.0129 atom% for Nd^{3+}. Then the Nd^{3+} concentration is estimated to be 1.08 10^{19} ions/cm^3. The results of the spectroscopic investigations are presented in the next paragraph.

3. Spectroscopy

3.1. Room temperature spectroscopic properties

The absorption spectra of a BIBO:Nd sample have been recorded with a Perkin-Elmer spectrophotometer. The light was polarized along the 3 principal X, Y, Z-axes of the optical indicatrix. The thickness of the sample was 0.288 cm for X-polarization and 0.467 cm for Y and Z-polarizations. The absorption coefficients (cm^{-1}) are depicted in Fig. 1 and we can see that the more intense peaks correspond to transitions from the ground state towards the $^4F_{5/2}$-$^2H_{9/2}$ (800 nm), $^4F_{7/2}$-$^4S_{3/2}$ (750 nm), $^4G_{5/2}$-$^2G_{7/2}$ (590 nm) levels. The low concentration of the sample is responsible for the noise all over the spectra.

Neverthless, the Judd-Ofelt treatment extended to anisotropic crystals was attempted [11].

The integrated absorption coefficient α_{iq} of the *i*th absorption band in the q polarization (i. e. X, Y, Z) is related to the P_{iq} oscillator strength :

$$P_{iq}^{(\exp)} = \frac{mc^2}{\pi e^2 \lambda^2 \rho} \int \alpha_{iq}(\lambda) d\lambda \qquad (1)$$

where ρ is the Nd concentration (ions/cm^3).

On the other hand, the oscillator strengths of the electric dipole transitions can be obtained theoretically from three sets of Judd-Ofelt parameters $\Omega_{t,q}$ (t=2, 4, 6) for the three q polarizations:

$$P_{iq}^{(th)} = \frac{(n_i^2+2)^2 8\pi^2 m\nu_i}{9n_i(2J+1)h} \sum_{t=2,4,6} \Omega_{tq} \left| \langle 4f^n[LS]J \| U^{(t)} \| 4f^n[L'S']J' \rangle \right|^2 \qquad (2)$$

where n_i is the index of refraction, ν_i is the centre frequency of the *i*-th absorption band, J=9/2 is the ground state angular momentum. In expression (2) the reduced matrix elements of tensor operators $U^{(t)}$ of rank t are tabulated in literature [12].

Seven experimental oscillator strengths have been fitted with the theoretical expression (2) in each polarization. The results are given in Table 1. The Ω_2 paramater was found close to zero for all the polarizations but slightly negative for X and Y polarizations. We think that this unphysical sign was due to the noise of the absorption spectra which results in difficulties to establish the baselines. So, for X and Y polarisations we have fixed Ω_2=0 and we did the fit by adjusting Ω_4 and Ω_6. Finally, we determined the Judd-Ofelt parameters to be $\Omega_{2X}=0$ cm^2 , $\Omega_{4X}=0.556\times10^{-20}$ cm^2, $\Omega_{6X}=0.227\times10^{-20}$ cm^2, $\Omega_{2Y}=0$ cm^2, $\Omega_{4Y}=0.307\times10^{-20}$ cm^2, $\Omega_{6Y}=0.177\times10^{-20}$ cm^2, $\Omega_{2Z}=0.069\times10^{-20}$ cm^2, $\Omega_{4Z}=0.433\times10^{-20}$ cm^2, $\Omega_{6Z}=0.117\times10^{-20}$cm^2.

The root mean square deviations (r. m. s.) defined by:

$$r.m.s. = \left[\frac{\sum_{i=1}^{7} (P_{iq}^{(\exp)} - P_{iq}^{(th)})^2}{number\ of\ bands\ fitted} \right]^{1/2} \qquad (3)$$

are 5.5×10^{-8} , 1.0×10^{-7} and 3.7×10^{-8} for X, Y, Z-polarizations respectively.

Table 1. Experimental (Pexp) and theoretical (Pth) oscillator strengths (x 10^6) of the transitions from the $^4I_{9/2}$ ground state for X, Y, Z-polarizations

Level	wavelength [nm]	Pth X-pol.	Pexp X-pol.	Pth Y-pol.	Pexp Y-pol.	Pth Z-pol.	Pexp Z-pol.
$^4F_{7/2}+^4S_{3/2}$	750	1.25	1.23	0.96	0.92	0.8	0.8
$^4F_{9/2}$	681	0.11	0.16	0.082	0.11	0.08	0.058
$^2H_{11/2}$	628	0.033	0.033	0.023	0.012	0.024	0.02
$^4G_{5/2}+^2G_{7/2}$	587	3.12	3.08	1.79	1.72	3.47	3.47
$^4G_{9/2}+^4G_{7/2}+^2K_{13/2}$	525	1.61	1.70	0.98	1.13	1.41	1.39
$^2G_{9/2}+^2D_{3/2}+^4G_{11/2}+^2K_{15/2}$	470	0.33	0.38	0.203	0.34	0.28	0.30
$^2P_{1/2}+^2D_{5/2}$	431	0.34	0.32	0.2	0.17	0.29	0.35

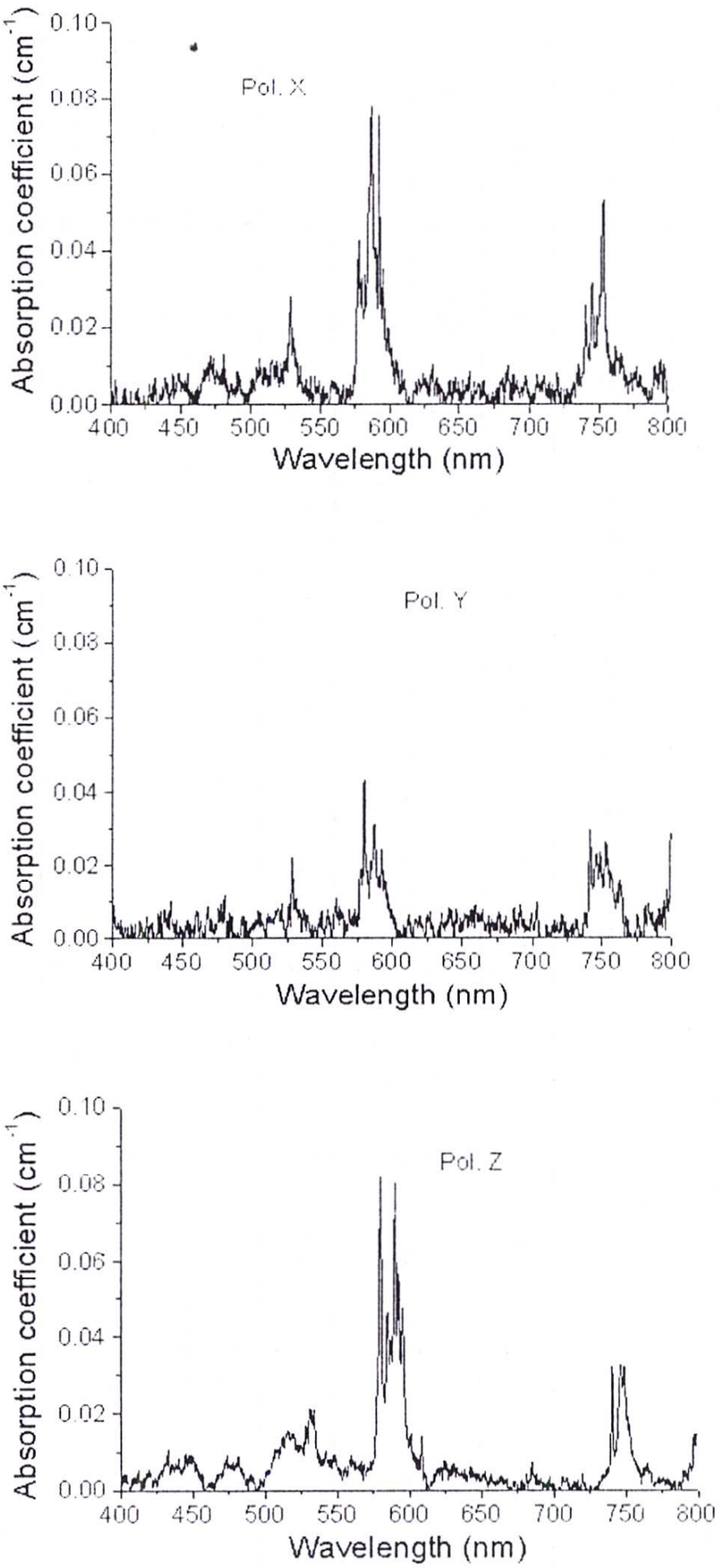

Fig. 1. Absorption spectra of BIBO:Nd^{3+} for light polarization along X (a), Y (b), Z (c) principal axes of the optical indicatrix

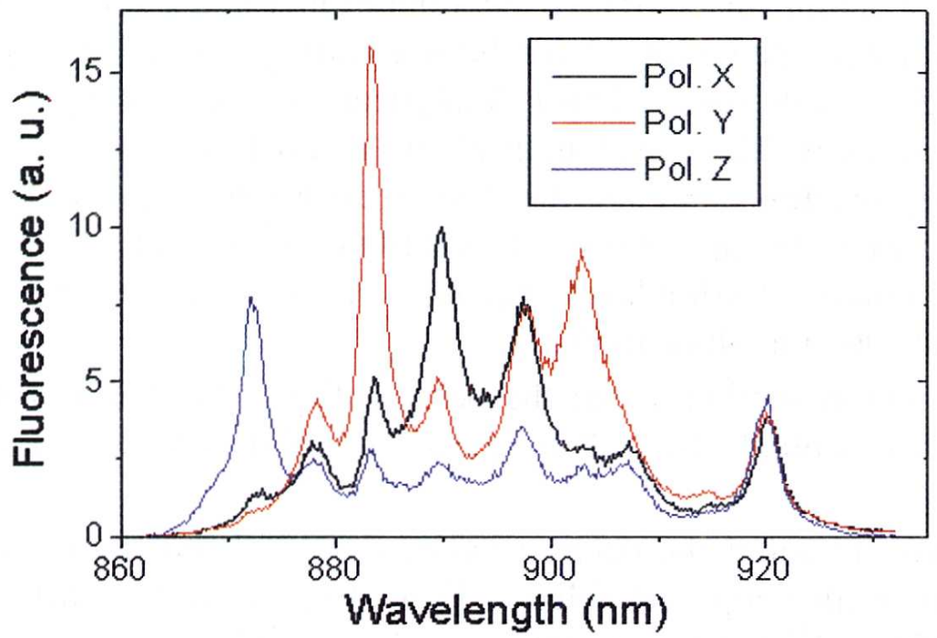

Fig. 2. Fluorescence spectra of BIBO:Nd^{3+} corresponding to the $^4F_{3/2} \rightarrow {}^4I_{9/2}$ transition for light polarization along X, Y, Z principal axes of the optical indicatrix

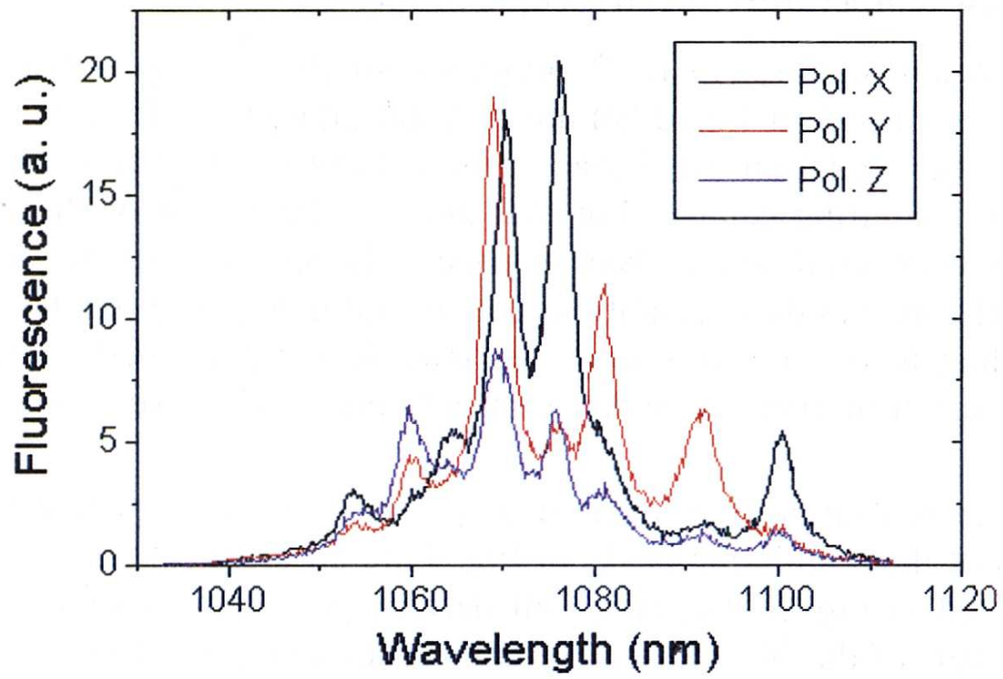

Fig. 3. Emission cross-section of BIBO:Nd^{3+} fluorescence corresponding to the $^4F_{3/2} \rightarrow {}^4I_{11/2}$ transition for light polarization along X, Y, Z principal axes of the optical indicatrix

The polarized emission spectra corresponding to the $^4F_{3/2} \rightarrow {}^4I_{9/2}$ and $^4F_{3/2} \rightarrow {}^4I_{11/2}$ transitions are represented in fig. 2 and 3 respectively. They were recorded with a Hammamatsu R1767 photomultiplier and a Jobin-Yvon HRS2 monochromator equipped with a 1 μm blazed grating, under pulsed excitation in the $^4F_{7/2}+{}^4S_{3/2}$ levels with a Laser Analytical dye laser pumped by a BM Industries YAG laser. The wavelength of the monochromator was calibrated with a mercury spectral lamp and the fluorescence intensities were corrected from the response of the apparatus. The Judd-Ofelt treatment has been used to calculate the polarized stimulated emission cross-section of the $^4F_{3/2} \rightarrow {}^4I_{9/2}$ transition near 1060 nm given in Fig. 3.

We shall see in section 4 that the peak in Fig. 3 located at 1069 nm in Y-polarization is suitable for self-frequency doubling and type I frequency mixing.

Finally we measured the decay time of the 1069 nm fluorescence with a 9410 Lecroy oscilloscope. Its value is 53 μs, to be compared with the value 98 μs in GdCOB:Nd^{3+} at low concentration [13] and 60 μs in NYAB [14]. The rather short lifetime in BIBO is probably explained by a non-radiative de-excitation from the $^4F_{3/2}$ level towards the immediately lower $^4I_{15/2}$ level: the calculated radiative lifetime is 1180 μs but nevertheless, by working sufficiently above the laser threshold, we expect that the quantum yield of the laser emission still remains close to unity.

3.2. Low temperature spectroscopic properties

The low temperature (18 K) fluorescence spectra were recorded from the sample located inside a liquid-helium cryostat equipped with a temperature controller. The excitation was broad spectral band in order to excite all the existing Nd^{3+} emitting centres. For that purpose the mirror of the dye laser oscillator was covered with a sheet of paper. The spectrum of the $^4F_{3/2} \rightarrow {}^4I_{11/2}$ transition obtained in these conditions is depicted in Fig. 4. It exhibits 6 peaks corresponding to the 6 Starks sublevels (two-fold degenerated) of the $^4I_{11/2}$. So, in this spectrum there is evidence of only one kind of Nd^{3+} emitting centre.

The high resolution laser excitation spectra (0.04 cm^{-1} spectral bandwidth) of each of the 6 emission peaks of Fig. 4 are all identical and one of them is represented in Fig. 5. The two well defined peaks correspond to the two Stark sublevels of the $^4F_{3/2}$. Laser excitation with a high resolution in the two peaks of Fig. 5 leads to emission spectra identical to the one obtained previously (Fig. 4) under broad band excitation, with six well defined peaks. So, once more, there is evidence of only one kind of Nd^{3+} emitting centre in BIBO.

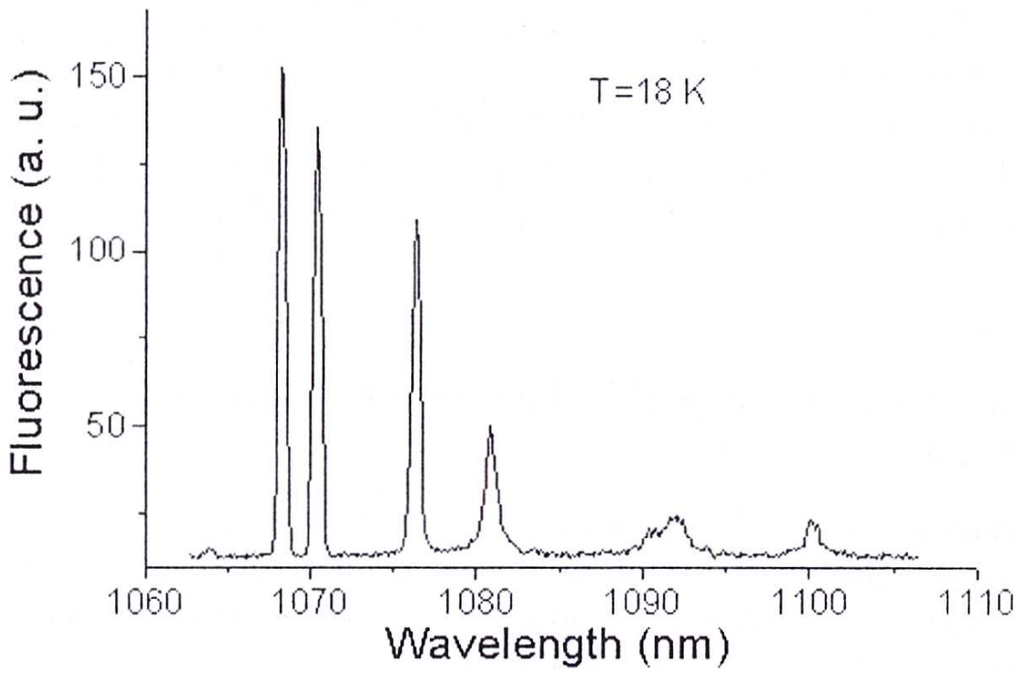

Fig. 4. Low temperature fluorescence spectrum of BIBO:Nd^{3+} corresponding to the $^4F_{3/2} \rightarrow {}^4I_{11/2}$ transition (unpolarized light)

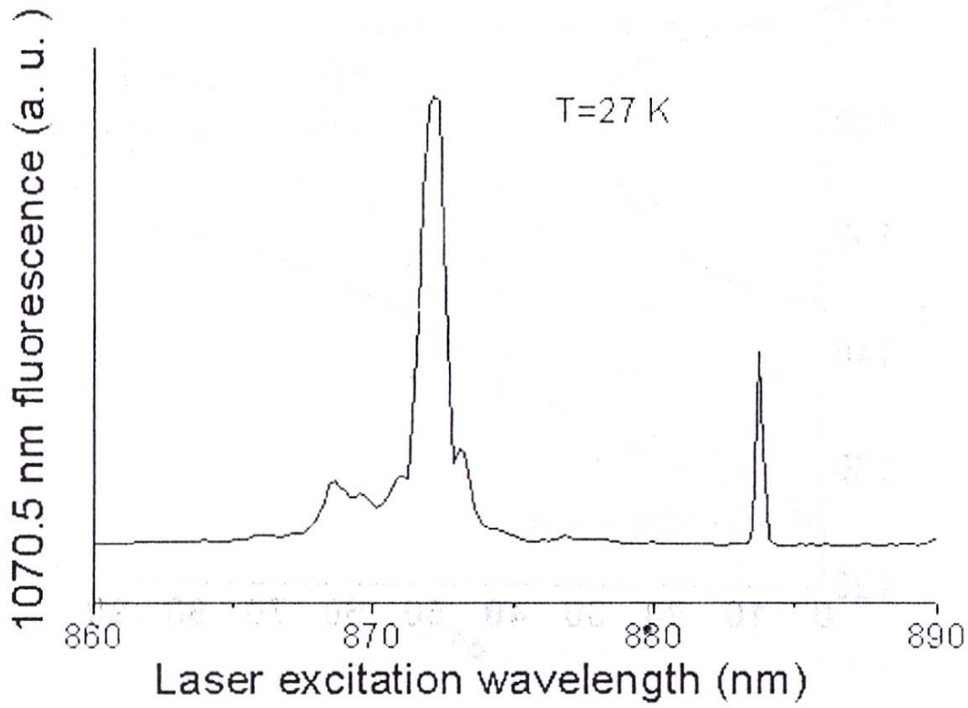

Fig. 5. Low temperature laser excitation spectrum of the 1070.5 nm emission line in BIBO:Nd^{3+} corresponding to the $^4F_{9/2} \rightarrow {}^4F_{3/2}$ transition (unpolarized light)

So, our low temperature measurements suggest that the Nd^{3+} ions substitute the sixfold coordinated Bi^{3+} cations in BIBO. This is reasonable since their ionic radius are close. Let us notice that this conclusion is valid for our low Nd^{3+} concentrated sample and possibly, in higher concentrated crystals several non-equivalent Nd^{3+} sites could appear, revealed by more peaks in Fig. 5. Let us add that the $^4F_{3/2}$ lifetime was measured to be 48 μs at 28 K.

4. Evaluation of Nd^{3+}-doped BiB_3O_6 as a new potential self-active laser crystal

It is nowadays a well established fact [5] that frequency conversion can be achieved in BIBO by the mean of three-wave nonlinear optical interactions. In this section we restrict our purpose to Type I collinear interactions, based on the following phase matching condition:

$$\omega_1 n_1^{+}(\theta,\varphi)+\omega_2 n_2^{+}(\theta,\varphi)=\omega_3 n_3^{-}(\theta,\varphi) \tag{4}$$

In (4) the waves propagate in the (θ, ϕ) direction and the upper sign + or – refers to the highest or the lowest (respectively) value of the refractive index.

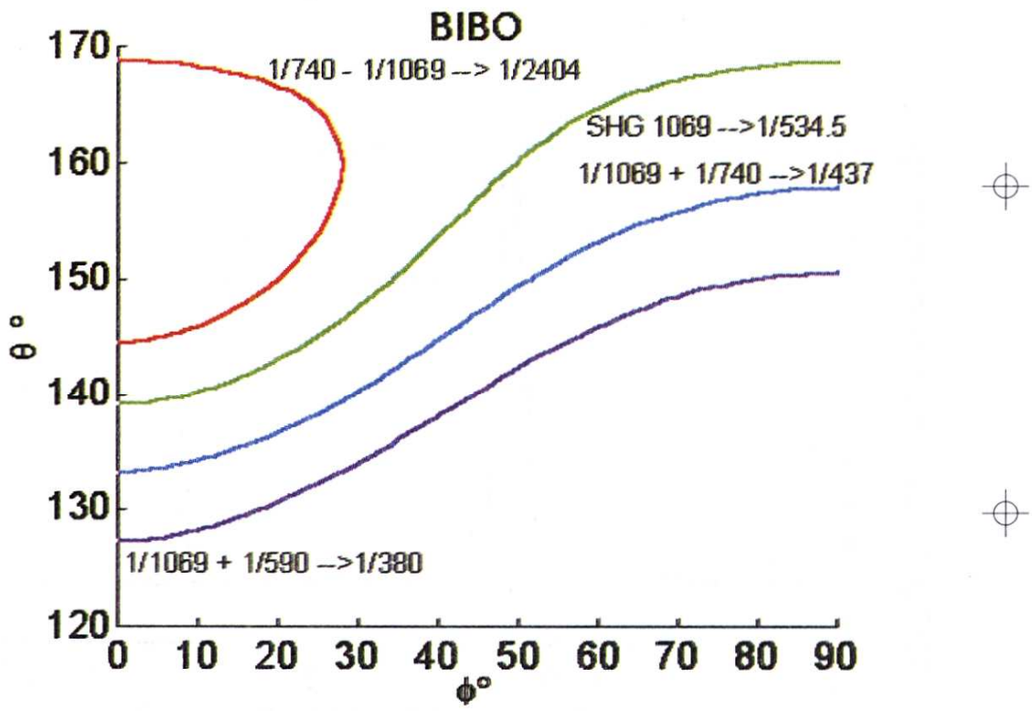

Fig. 6. Calculated phase matching directions for different self-frequency conversion processes in BIBO:Nd^{3+}

More, we want to determine the possibility that BIBO:Nd^{3+} works as a self-frequency conversion laser crystal implying the more intense transition: $^4F_{3/2} \rightarrow {}^4I_{11/2}$ in the 1040 – 1100 nm spectral range. This means that one of the waves in the condition (4), let us call it ω_2, has to be the laser wave generated by the Nd^{3+} ions located inside the BIBO lattice. The choice of ω_2 for our evaluation must be in agreement with the polarized emission spectra in Fig. 3 and all the main peaks have to be considered. We have found (using the procedure described below) that the *more favourable one* to get simultaneously high intensity of fluorescence in the right polarization and high yield of frequency conversion in the directions where (4) is satisfied, is the peak appearing in Y-polarisation in Fig. 3 at λ_2=1069 nm. So in the evaluation described here, we have fixed ω_2 accordingly.

In the case of self-frequency doubling, the pumping beam in the Nd^{3+} absorption lines has no role in relation (4) and ω_3 corresponds to the self-doubled wave of the ω_2 laser. In the case of the self-sum frequency mixing, the pumping wave in the Nd^{3+} absorption lines has also in (4) the role of ω_1. The Nd^{3+} absorption levels chosen in the present evaluation are the $^4F_{7/2}$-$^4S_{3/2}$ (at 740 nm) and the $^4G_{5/2}$-$^2G_{7/2}$ (at 590 nm) levels. These processes generate radiation at 437 and 380 nm corresponding to ω_3 in (4) and have been demonstrated in NYAB [15,16], GdCOB:Nd [17] and NGAB [18]. In the case of self-difference frequency mixing, the pumping wave in the Nd^{3+} absorption lines has in (4) the role of ω_3 and the Nd^{3+} absorption level has been chosen to be the $^4F_{7/2}$-$^4S_{3/2}$ (at 740 nm) level. This process produces radiation at 2404 nm as ω_1 in (4). To summarize, we evaluate in the following the self-frequency conversion processes in BIBO:Nd^{3+}:

1/1069+1/1069→1/534.5 (green)

1/1069+1/740→1/437 (blue)

1/1069+1/590→1/380 (UV)

1/740-1/1069→1/2404 (IR)

For each of the self-frequency conversion processes cited above, the phase matching directions (θ, ϕ — generally out of the principal planes) have been calculated using the data for the Sellmeier equations from [5]. The results are visualized in Fig. 6.

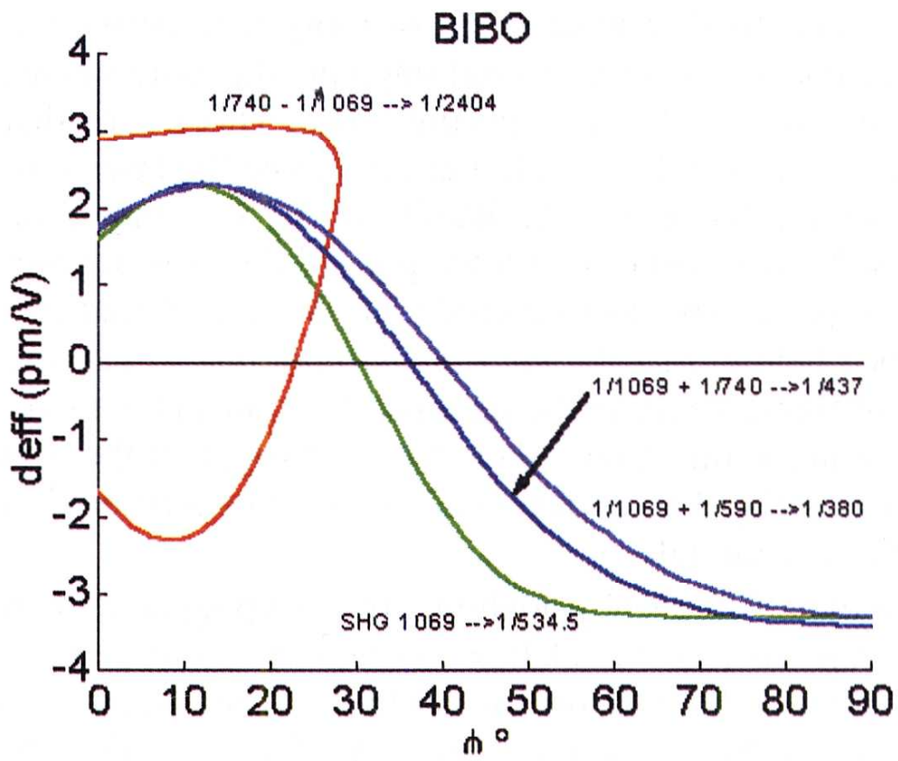

Fig. 7. Calculated effective nonlinear coefficient for different self-frequency conversion processes in BIBO:Nd^{3+}

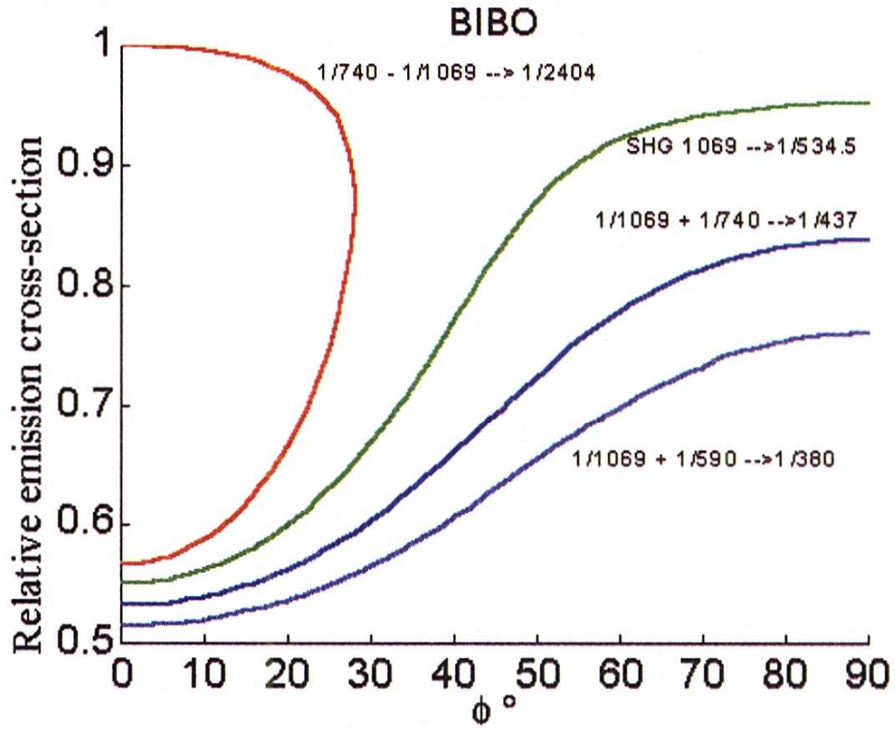

Fig. 8. Ratio $\sigma(\theta, \phi)/\sigma_y$ at 1069 nm (σ_y=1.9 10^{-20} cm^2) calculated for different self-frequency conversion processes in BIBO:Nd^{3+}

Then for each phase matching direction of the considered processes, the effective nonlinear optical coefficient has been calculated. As the example of self-frequency doubling we used the well-known formula:

$$d_{eff} = p_i(2\omega_2) d_{ijk}\, e_j(\omega_2)\, e_k(\omega_2) \tag{6}$$

where $e_i(\omega_2)$is the ith component of the unit vector of the electric field of the laser wave and $p_i(2\omega_2)$ is the ith component of the unit vector of the polarization. A corresponding formula was used for sum and difference frequency mixing. The d_{ijk} in (5) are extracted from [5]. The results of the calculations are represented in Fig. 7.

Finally, for each phase matching direction (θ, ϕ) of the considered processes, the effective laser emission cross-section $\sigma(\theta, \phi)$ at 1069 nm in the right polarization (the one which propagates with n_2^+ refractive index) has to be estimated. For electric-dipole transition in a biaxial crystal, we can use the relation:

$$\sigma(\theta,\varphi)=\frac{\sigma_x\sigma_y\sigma_z}{\sqrt{\sigma_y^2\sigma_z^2e_x^2+\sigma_x^2\sigma_z^2e_y^2+\sigma_x^2\sigma_y^2e_z^2}} \tag{6}$$

where $\sigma_{X,Y,Z}$ are the emission cross-sections for X, Y, Z-polarizations and $e_{X,Y,Z}$ are the components of the unit vector or the electric field of the laser wave ω_2 propagating in the (θ, ϕ) direction. We have extracted from the emission spectra in Fig. 3 the ratio $\sigma(\theta, \phi)/\sigma_y$ at 1069 nm to visualize the directions of the highest laser efficiency, keeping in mind that σ_y=1.9 10^{-20} cm^2 at 1069 nm. The result is given in Fig. 8.

Inspection of Fig. 6 – 7 – 8 shows that for the self-doubling and self-sum mixing processes, the most favourable directions are close to ϕ=90°: the highest absolute value of the nonlinear optical coefficient d_{eff} is obtained simultaneously with the highest value of the laser emission cross-section. In the case of the self-difference frequency process, the same coincidence occurs close to the direction ϕ=0°, θ=170°.

Conclusion

We present in this work an evaluation of a new *potential* self-frequency conversion laser crystal: BIBO:Nd^{3+}, based on spectroscopic measurements and data on linear and nonlinear dielectric susceptibility. One main point is that the measured Nd^{3+} concentration in the crystal remains low and prevents up to now laser oscillation. Progress are still to be made to increase this con-

centration. The crystal exhibits only one kind of Nd^{3+} emitting centre, without disorder, which is often a favourable situation for getting high emission cross-section in a laser material. At room temperature, peaks stand out from the emission spectra at least in X and Y-polarisations with emission cross-section close to 2 10^{-20} cm^2, which is the same order of magnitude as the famous Gd-COBNd^{3+} [17]. Concerning the self-doubling and self-sum mixing processes, the most favourable directions are $\phi=90°$ (YZ-plane) or close. In the case of the self-difference frequency process, the most favourable directions are $\phi=0°$ (XZ-plane or close) , $\theta=170°$.

Acknowledgements:

Dr. A. Yoshikawa, from Tohoku University, is gratefully acknowledged for EPMA analysis.

References

[1] J. Lierbertz, *Prog. Crystal Growth Charact*, 6 (1983) 361.

[2] P. Becker, J. Liebertz, L. Bohaty, „J. Crystal Growth", 203 (1999) 149.

[3] V. R. Frohlich, L. Bohaty, J. Liebertz, „Acta Cryst." C40 (1984) 343.

[4] H. Hellwig, J. Liebertz, L. Bohaty, „Solid State Comm." Vol. 109 n°4 (1999) 249.

[5] H. Hellwig, J. Liebertz, L. Bohaty, „J. Applied Phys." Vol. 88 n°1 (2000) 240.

[6] D. Xue, K. Betzler, H. Hesse, D. Lammers, „Solid State Comm." 114 (2000) 21.

[7] P. Becker, C. Wickleder, „Cryst. Res. Technol." 36–1 (2001) 27.

[8] A. Brenier, J. Lumin. 91 (2000) 121–132.

[9] E.M. Levin and C.L. McDaniel, „J. Am. Ceram. Soc.", Vol. 45, n°8 (1962) 355.

[10] A. Majchrowski, in „Supermaterials", R. Cloots et al. (eds.), Kluwer Academic Publishers (2000) 101.

[11] H. Dai, O.M. Stafsudd, „J. Phys. Chem. Solids" vol. 52 n°2 (1991) 367–379.

[12] W.T. Carnall, H. Crosswhite, H.M. Crosswhite, Special Report 1977, Chemistry Division, Argonne National Laboratory (Argonne, IL,USA).

[13] F. Mougel, G. Aka, A. Kahn-Harari, H. Hubert, J.M. Benitez, D. Vivien, „Opt. Materials" 8 (1997) 161.

[14] Z. Luo, „Progress in Natural Science", vol. 4 n°4 (1994) 504.

[15] A. Brenier, G. Boulon, D. Jaque, J. Garcia Solé, „Opt. Mater." 13 (1999) 311.

[16] A. Brenier, G. Boulon, J. Lumines. 86 (2000) 125.

[17] F. Mougel, G. Aka, A. Kahn-Harari, D. Vivien, Op. Mater." 13 (1999) 293.

[18] A. Brenier; Chaoyang Tu, Minwang Qiu, Aidong Jiang, Baichang Wu, Jianfu Li, „J. Opt. Soc. Am." B vol. 18 n°8 (2001) 1.

A. BRENIER, I.V. KITYK, J.BERDOWSKI, A. MAJCHROWSKI

Nd^{3+}-doped BiB_3O_6 (BIBO) as a new potential self-frequency conversion laser crystal

Summary

Abstract: We present at room temperature emission and absorption spectra of new-synthesized Nd^{3+}-doped BiB_3O_6 (BIBO) in X, Y, Z-polarisations. The measured Nd^{3+} concentration in the crystal remains low ($1.08\ 10^{19}$ ions/cm^3) and prevents up to now laser oscillation. The Judd-Ofelt analysis was performed with the results: $\Omega_{2X}=0$ cm^2, $\Omega_{4X}=0.556\times10^{-20}$ cm^2, $\Omega_{6X}=0.227\times10^{-20}$ cm^2, $\Omega_{2Y}=0$ cm^2, $\Omega_{4Y}=0.307\times10^{-20}$ cm^2, $\Omega_{6Y}=0.177\times10^{-20}$ cm^2, $\Omega_{2Z}=0.069\times10^{-20}$ cm^2, $\Omega_{4Z}=0.433\times10^{-20}$ cm^2, $\Omega_{6Z}=0.117\times10^{-20}$ cm^2. The highest emission cross-section near 1079 nm is $2.2\ 10^{-20}$ cm^2. The $^4F_{3/2}$ emission lifetime is 53 μs. Low temperature spectroscopy reveals that there is only one kind on Nd^{3+} emitting centre which substitutes Bi^{3+} cations. We evaluate the ability of the material to be a self-frequency conversion laser crystal by calculating the phase matching directions, the effective nonlinear optical coefficients and the effective emission cross-sections for self-frequency doubling, self-sum and difference frequency mixing. We have found that the emission peak at 1069 nm existing mainly for Y-polarization was the most favourable with directions of propagations in the YZ-plane ($\phi=90°$) for self-sum frequency mixing and in the XZ-plane ($\phi=0°$) for the self-difference frequency mixing. For these directions the effective nonlinear optical coefficient (up to 3.2 pm/V) and the effective emission-cross section have simultaneously the highest values.